

Solar neutrino problem in light of super-Kamiokande data

S UMA SANKAR

Department of Physics, Indian Institute of Technology, Mumbai 400 076, India

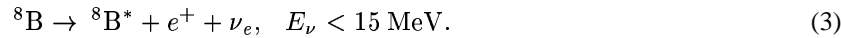
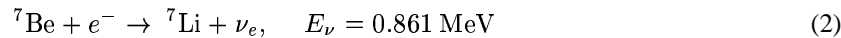
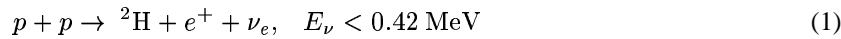
Abstract. I discuss the status of the accepted solutions to the solar neutrino problem in light of the super-Kamiokande data.

Keywords. Solar neutrinos; super-Kamiokande.

PACS Nos 14.60 Pq; 14.60 St

Solar neutrino problem is the oldest of the neutrino puzzles which cannot be accounted for by the standard model. During the last ten years data from various solar neutrino experiments [1–4] have reached such a good accuracy that astrophysical solutions are ruled out. We must invoke neutrino physics beyond the Standard Model, in particular neutrino oscillations to obtain a satisfactory solution to the solar neutrino problem. Recent super-K results on atmospheric neutrinos, in particular on the up-down asymmetry in atmospheric muons, gave a strong impetus to the study of neutrino oscillations [5]. The super-K data on solar neutrinos put new constraints on the previously allowed solutions and restrict them further [6].

The pp chain is the dominant energy producing cycle in the sun. In this chain, neutrinos are produced in the following reactions:



These reactions are the dominant sources of signals in the solar neutrino detectors. The pp reaction in eq. (1) is the first in the chain of energy producing reactions in the sun. From the measurement of the solar luminosity, this reaction rate can be determined quite accurately and the flux of pp neutrinos can be predicted with good precision. The predictions for the ν_e fluxes from ${}^7\text{Be}$ and ${}^8\text{B}$ reactions can not be predicted very accurately because the concentrations of ${}^7\text{Be}$ and ${}^8\text{B}$ reactions are not well known. These nuclei are produced in the following reactions:





Particles in the solar core have kinetic energies of a few KeV. In the lab, the rates for the above reactions are measured where the energies of the initial particles are a few MeV. To obtain the rates for these reactions, in the conditions of the solar core, involves extrapolation from laboratory measurements. The uncertainties in these calculations can be quite large, particularly for the ${}^8\text{B}$ production reaction in eq. (5) [7].

The solar neutrino experiments are of three types which can be characterized by the medium used for neutrino detection. These are gallium (GALLEX and SAGE), chlorine (Homestake) and water (Kamiokande and super-Kamiokande). Gallium and chlorine experiments are radiochemical experiments in which the neutrino induces an inverse beta decay. The signal is measured by counting the number of germanium (for gallium experiments) or argon (for chlorine experiment) atoms in the detector at regular intervals. Due to this procedure, these experiments see only time averaged signal and are not capable of determining the energy of the incoming neutrino. Kamiokande and super-Kamiokande detect the Cerenkov light emitted by the electron in the reaction $\nu + e \rightarrow \nu + e$. Hence these experiments detect the neutrinos in real time and by measuring the energy of the scattered electron, they can determine the energy of the incoming neutrino. The $\nu_e - e$ scattering can occur via both charged current (CC) and neutral current (NC), whereas the $\nu_\mu - e$ (or $\nu_\tau - e$) scattering can occur only via NC. The NC cross-section is about one fifth of the CC cross-section [8]. In analysing the data of Kamiokande and super-K, the NC contribution to signal from the oscillated neutrino species should be taken into account.

The predictions for the neutrino fluxes from various reactions are calculated using the standard solar model (SSM) of Bahcall and Pinsonneault [9]. Combining these fluxes with the detector characteristics, we can calculate the signal rates for each of the detectors. The thresholds and the SSM predictions for the signal rates for various experiments are shown in the table 1 [10].

The sum of the three specific rates do not add up to the total expected rate because there are small contributions to the total rate from CNO cycle. We will not explicitly consider the CNO neutrinos here. The rates for Kamiokande and super-Kamiokande are given in units of $10^6 \text{ cm}^{-2}\text{s}^{-1}$. The unit for other rates, the solar neutrino unit (SNU), is 10^{-36} events per target atom per second.

In table 1, the uncertainty in the SSM prediction for the water Cerenkov detectors, which are sensitive only to ${}^8\text{B}$ flux, is quite large. However, this does not include the uncertainty in the extrapolation procedure needed to calculate the ${}^8\text{B}$ concentration in the sun. If one uses an extrapolation procedure different from the one used by Bahcall and Pinsonneault, the prediction for ${}^8\text{B}$ flux goes up by 20% [10]. This fact must be taken into account when we compare the data with the predictions of the SSM.

The signal rates measured by the different experiments are given in table 2. In table 2, only the experimental errors are quoted in the third column.

We see that all the experiments see a neutrino flux that is less than that expected from the SSM. Moreover, the suppression seen by each experiment is different. Since different experiments are sensitive to neutrinos of different energies, the suppression seems to be a function of neutrino energy. It is impossible to obtain such a suppression by modifying the solar model, even if we assume that one of the experiments is wrong [11]. Hence we need to invoke new physics for neutrinos to satisfactorily explain all the solar neutrino data.

Neutrino oscillations provide a very good solution to the solar neutrino problem. If the ν_e produced in the solar core oscillates into another flavour during its travel to earth,

Table 1.

Experiment	Threshold	pp rate	${}^7\text{Be}$ rate	${}^8\text{B}$ rate	Total
GALLEX, SAGE	0.233 MeV	70 SNU	35 SNU	15 SNU	129^{+8}_{-6}
Homestake	0.814 MeV	0	1.1 SNU	6.1 SNU	7.7 ± 1
Kamiokande	7.5 MeV	0	0	5.15	$5.15^{+1.0}_{-0.7}$
Super-Kamiokande	6.5 MeV	0	0	5.15	$5.15^{+1.0}_{-0.7}$

Table 2.

Experiment	Measurement	Measurement/Prediction
GALLEX	77.5 ± 7.5 SNU	0.6 ± 0.06
SAGE	66.6 ± 7.9 SNU	0.52 ± 0.06
Homestake	2.56 ± 0.2 SNU	0.33 ± 0.029
Kamiokande	2.8 ± 0.38	0.54 ± 0.07
Super-Kamiokande	2.44 ± 0.085	0.474 ± 0.020

then the measured rate will be smaller than the SSM predicted rate. The survival probability P_{ee} for a ν_e produced in the sun to be detected as ν_e on earth is given by [12]

$$P_{ee} = 1 - \sin^2 2\theta \sin^2 \left(1.27 \frac{\Delta m^2 L}{E_\nu} \right). \quad (6)$$

In the above equation, Δm^2 is in eV^2 , L is in meters and E_ν is in MeV. Equation (6) is derived under the assumption that only two flavours, ν_e and ν_μ mix with each other and θ is the mixing angle. $\Delta m^2 = m_2^2 - m_1^2$, where m_1 and m_2 are mass eigenvalues of the two mass eigenstates which arise out of $\nu_e - \nu_\mu$ mixing. L is the sun–earth distance which is about 10^{11} meters. In the case of the radiochemical experiments, the ratio of measured rate to the predicted rate directly gives P_{ee} . In the case of the water Cerenkov detectors, we should subtract the NC contribution to the signal to determine P_{ee} . With this subtraction, we get $P_{ee} = 0.45 \pm 0.07$ for Kamiokande and $P_{ee} = 0.37 \pm 0.02$ for super-K. As mentioned before, data in table 2 do not seem to allow P_{ee} to be independent of energy. Since L is large, we see from eq. (6) that the energy dependent term oscillates very fast if Δm^2 is also large. In such cases it averages out to 0.5 when the variations in L and E_ν are taken into account. Hence large values of $\Delta m^2 (\geq 10^{-4} \text{ eV}^2)$, which are needed for a solution of the atmospheric neutrino problem [5], are ruled out because they lead to energy independent suppression of solar neutrino flux.

Wolfenstein considered the effect of dense solar matter on the propagation of neutrinos [13]. Since ν_e interacts with electrons both via CC and NC, whereas ν_μ interacts only via NC, this propagation leads to an extra term for ν_e in the (mass)² matrix. The matter term is given by

$$A = 0.76 \rho E \times 10^{-7}, \quad (7)$$

where A is in eV^2 , ρ the matter density is in g/cc and E the neutrino energy is in MeV . It was realized by Mikheyev and Smirnov that, for appropriate values of Δm^2 , a resonance could occur if

$$\Delta m^2 \cos 2\theta = A \quad (8)$$

which can lead to large oscillation probability, even if the original mixing angle is small [14,15]. If we calculate P_{ee} , taking the MSW effect into account [16,17], and fit the data on overall suppression, we obtain two allowed regions in the parameter space [10]:

$$\begin{aligned} \text{Small angle region : } \Delta m^2 &\simeq 5.4 \times 10^{-6} \text{ eV}^2, \quad \sin^2 2\theta \simeq 6.0 \times 10^{-3}, \\ \text{Large angle region : } \Delta m^2 &\simeq 1.8 \times 10^{-5} \text{ eV}^2, \quad \sin^2 2\theta \simeq 0.76. \end{aligned}$$

The graphs of P_{ee} for the small and the large angle solutions are shown in figures 1 and 2 respectively. In the case of the small angle solution, the pp flux is unaffected, ${}^7\text{Be}$ flux is completely suppressed and the suppression of ${}^8\text{B}$ flux has a strong energy dependence with P_{ee} increasing rapidly in the range 5 – 10 MeV. In the case of the large angle solution P_{ee} for pp flux is about 0.6, for ${}^7\text{Be}$ flux it is 0.5 and for ${}^8\text{B}$ flux it is energy independent with a value of about 0.25.

The small angle solution gives better fit to the data on overall suppression than the large angle solution if one uses the predictions of Bahcall–Pinsonneault [9]. However, if ${}^8\text{B}$ flux is calculated by the other extrapolation procedure which leads to a higher prediction of the ${}^8\text{B}$ flux, then the large angle solution gives a better fit to the data than the small angle solution [10]. Because of the large uncertainty in the prediction of ${}^8\text{B}$ flux, one should look for signals in the ${}^8\text{B}$ data, which are independent of the prediction for the overall flux. Two such signals are

- Day–night asymmetry
- Electron spectrum distortion

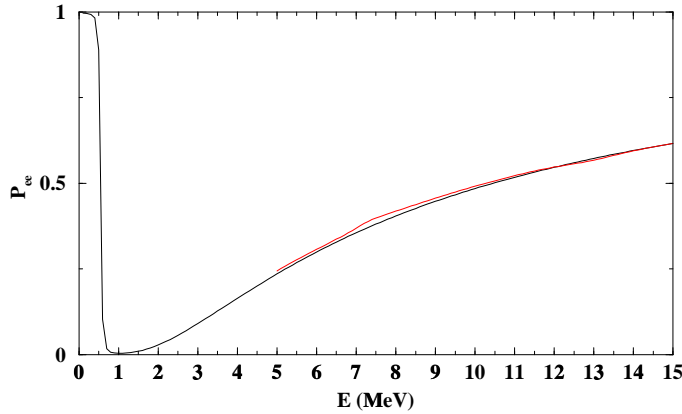


Figure 1. Day (thick) and night (thin) survival probabilities as functions of energy for the MSW small angle solution. The night probability is obtained by averaging over the exposure times for different lengths of traversal.

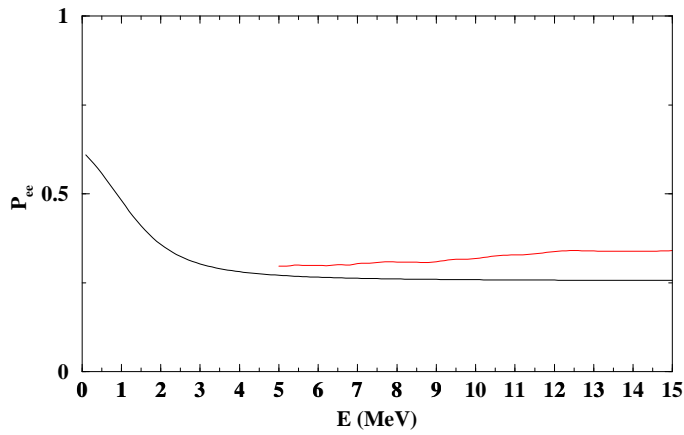


Figure 2. Day (thick) and night (thin) survival probabilities as functions of energy for the MSW large angle solution. The night probability is obtained by averaging over the exposure times for different lengths of traversal.

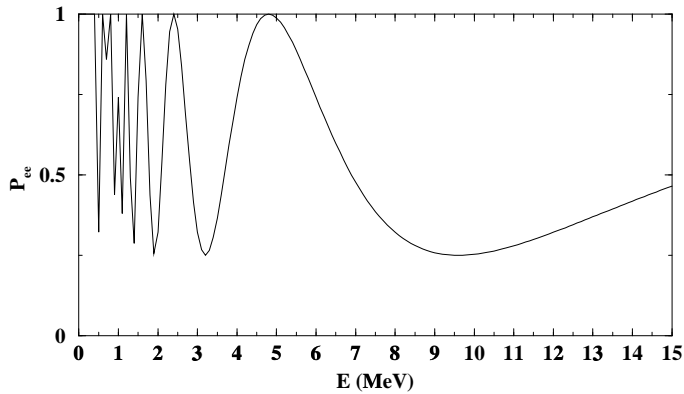


Figure 3. Survival probability as a function of energy for vacuum oscillation solution.

The day–night asymmetry can arise because the MSW effect can reconvert some of the oscillated neutrinos back to ν_e as they pass through the earth matter. Due to this, the signal is expected to be larger during night than during day. The ratio of night signal to day signal is independent of the prediction of overall ${}^8\text{B}$ flux and depends only on the neutrino parameters. In figures 1 and 2, P_{ee} for day is plotted as a thick line and P_{ee} for night is plotted as a thin line. In calculating the night probability, the actual density profile of earth is used and the exposure times for different lengths of traversal in earth are folded in [18]. In the case of the small angle solution, the day and the night survival probabilities are practically indistinguishable. In the case of the large angle solution, there is a discernible difference between the day and the night survival probabilities. This difference can lead to measurable day–night asymmetry. Kamiokande’s measurement of day–night asymmetry

is consistent with zero but, due to the limited number of events, the uncertainties are large. Super-K measured the day–night asymmetry to a very good precision. Their result is

$$A_{n-d} = \frac{N - D}{N + D} = 0.03 \pm 0.018(\text{stat}) \pm 0.004(\text{syst}), \quad (9)$$

where D is the day rate and N is the night rate [19]. Note that the systematic uncertainty is very small. The statistical error will go down with the collection of more data. Hence we can expect a very accurate measurement of A_{n-d} . The smallness of the day–night asymmetry rules out some of the parameter space, both in the small and large angle regions, that was allowed by overall rates. Though the present measurement of A_{n-d} is not capable of discriminating between the small and the large angle solutions, future, more precise measurements can.

The ^8B neutrinos are produced via a weak decay and have the usual three body decay spectrum. This spectrum is determined purely by the electroweak theory and is independent of the overall flux. From the neutrino spectrum we can calculate the expected spectrum of the scattered electrons in the water Cerenkov detectors. By comparing the measured electron spectrum to the calculated one, we can determine if the spectrum is distorted. Super-K measured the scattered electron spectrum in the energy range 6.5–20 MeV. The graph for the ratio of measured events in an energy bin to the number of expected events in the same bin is more or less flat in the energy range 6.5–12.5 MeV. Above 12.5 MeV the ratio is larger than the average value, though the error bars are large. From figure 1, we see that the P_{ee} for the small angle solution rises quite sharply. It increases from 0.25 at 6 MeV to 0.5 at 12 MeV. The spectrum of ν_e 's reaching the detector will be modulated by this P_{ee} and we expect a corresponding distortion in the electron spectrum. The fact that no such distortion is seen makes the small angle solution disfavoured though it can not be ruled out with the current statistics. The P_{ee} for the large angle solution is independent of energy above 2 MeV. Thus the flat electron spectrum observed by super-K can easily be accounted for by the large angle solution. The larger than average number of events seen above 12.5 MeV do pose a problem for the large angle solution. However, the large error bars in these bins do not make them statistically significant.

So far we have been discussing only solutions based on MSW effect. There is, however, another neutrino oscillation solution which is consistent with data. This is the vacuum oscillation solution with Δm^2 so small that less than one oscillation occurs between the sun and the earth for ^8B neutrinos with energy greater than 5 MeV. Since the diameter of earth is negligible compared to the sun–earth distance, there will not be any day–night effect for such oscillations. Assuming such vacuum oscillations, we can calculate rates for various experiments and also the electron spectrum. By comparing the data to these predictions we can determine the values for Δm^2 and $\sin^2 2\theta$ which fit the data the best. The best fit values are

$$\Delta m^2 = 6.5 \times 10^{-11} \text{ eV}^2 \quad \sin^2 2\theta = 0.75. \quad (10)$$

The P_{ee} for this solution is plotted in figure 3 as a function of neutrino energy. We see that for energies below 5 MeV, the oscillations are rapid and will be averaged out even over an energy bin of size 0.5 MeV. But above 5 MeV, the P_{ee} varies smoothly with energy and the rise of P_{ee} beyond 10 MeV can account for the larger values of measured to expected ratio that has been observed. However, in the energy range 5–10 MeV, the spectral distortion due to vacuum oscillations is quite different from that of both small and large angle solutions.

The energy threshold for super-K will soon be lowered to 5.5 MeV and the measurement of the spectrum from the smaller threshold will help us distinguish the vacuum solution.

In conclusion, the overall suppression measurement of super-K has not altered any of the allowed solutions. However, the good measurements of the day–night asymmetry and the scattered electron spectrum seem to disfavour the small angle solution and favour the large angle solution. With present uncertainties, though, both MSW solutions along with vacuum oscillation solution, remain viable. The day–night asymmetry will differentiate between the MSW small angle and large angle solutions. The spectral distortion, especially with the lower threshold of 5.5 MeV, can distinguish between all the three allowed solutions. More accurate measurements of these quantities, and the data from future solar neutrino experiments such as SNO and Borexino, will pin down the solution to the solar neutrino problem.

Acknowledgement

I thank the organizers for conducting this exciting workshop and for inviting me to give this talk.

References

- [1] B T Cleveland *et al*, *Astrophys. J.* **496**, 505 (1998)
- [2] Kamiokande Collaboration: Y Fukuda *et al*, *Phys. Rev. Lett.* **77**, 1683 (1996)
- [3] SAGE Collaboration: V Gavrin *et al*, in *Neutrino 96*, Proceedings of the XVII International Conference on Neutrino Physics and Astrophysics, Helsinki, edited by K Huitu, K Enqvist and J Maalampi (World Scientific, Singapore, 1997) p. 14
- [4] GALLEX Collaboration: P Anselman *et al*, *Phys. Lett.* **B342**, 440 (1995)
W Hampel *et al*, *Phys. Lett.* **B388**, 364 (1996)
- [5] Super-Kamiokande Collaboration: Y Fukuda *et al*, *Phys. Rev. Lett.* **81**, 1562 (1998)
- [6] Super-Kamiokande Collaboration: Y Fukuda *et al*, *Phys. Rev. Lett.* **81**, 1158 (1998); Erratum *ibid* **81**, 4279 (1998)
- [7] J N Bahcall, *Neutrino Astrophysics* (Cambridge University Press, Cambridge, 1989), Chapter 2
- [8] Ref. [7], Chapter 8
- [9] J N Bahcall, S Basu and M H Pinsonneault, *Phys. Lett.* **B433**, 1 (1998)
E Adelberger *et al*, *Rev. Mod. Phys.* **70**, 1265 (1998)
- [10] J N Bahcall, P I Krastev and A Yu Smirnov, *Phys. Rev.* **D58**, 096016 (1998)
- [11] N Hata, S Bludman and P Langacker, *Phys. Rev.* **D49**, 3622 (1994)
- [12] B Pontecorvo, *Zh. Eksp. Theor. Fiz.* **33**, 549 (1957); *JETP* **6**, 429 (1958); *ibid* **53**, 1717 (1967); *JETP* **26**, 984 (1968)
- [13] L Wolfenstein, *Phys. Rev.* **D17**, 2369 (1978)
- [14] S P Mikheyev and A Yu. Smirnov, *Yad. Fiz.* **42**, 1441 (1985); *Sov. J. Nucl. Phys.* **42**, 913 (1985); *Nuovo Cimento* **C9**, 17 (1986)
- [15] H A Bethe, *Phys. Rev. Lett.* **56**, 1305 (1986)
- [16] S Parke, *Phys. Rev. Lett.* **57**, 1275 (1986)
- [17] P Pizzocherri, *Phys. Rev.* **D36**, 2293 (1987)
- [18] Mohan Narayan, G Rajasekaran and Rahul Sinha, *Mod. Phys. Lett.* **A13**, 1915 (1998)
- [19] J N Bahcall, P I Krastev and A Yu. Smirnov, hep-ph/9905220